LA-UR-19-20523
Approved for public release; distribution is unlimited.

Title: MIS High Purity Plutonium Oxide Metal Oxidation Product MT1490 (SSR125): Final Report

Author(s): Veirs, Douglas Kirk
Stroud, Mary Ann
Martinez, Max A.
Carrillo, Alex
Berg, John M.
Narlesky, Joshua Edward
Worl, Laura Ann
Kulis, Jerzy

Intended for: Report

Issued: 2019-07-30 (rev.1)

MIS High Purity Plutonium Oxide Metal Oxidation Product MT1490 (SSR125): Final Report

Authors:

D. Kirk Veirs
Mary A. Stroud
Max A. Martinez (retired)
Alex Carrillo (retired)
John M. Berg
Joshua E. Narlesky
Laura Worl
Jerzy Kulis

MIS High Purity Plutonium Oxide Metal Oxidation Product MT1490 (SSR125): Final Report

Abstract

A high purity plutonium dioxide material from the Material Identification and Surveillance (MIS) Program inventory has been studied with regard to gas generation and corrosion in a storage environment. Sample MT1490 represents process plutonium oxides from several metal oxidation operations that are currently stored in 3013 containers. This study followed over time, the gas pressure of a sample with nominally 0.5 weight percent water in a sealed container with an internal volume scaled to 1/500th of the volume of a 3013 container. The sample was a mixture of as-received material, material calcined at 800°C and material calcined at 950°C. This material contained 87% plutonium with no major impurities. Gas compositions were measured periodically over a nine year period. The maximum observed gas pressure of 118 kPa was reached during the ninth year. The increase over the initial pressure of 95 kPa was primarily due to generation of nitrogen and hydrogen gas. Oxygen was a minor component of the headspace gas. At the completion of the study, the inner bucket showed signs of corrosion, including pitting, in the container material contact region.

Contents

Figures

Tables

Introduction

The Los Alamos National Laboratory (LANL) Shelf-life Surveillance project was established under the Material Identification and Surveillance (MIS) Program to identify early indications of potential failure mechanisms in 3013 containers.[1] Samples were taken from plutonium processes across the DOE complex. These "representative" materials were sent to LANL to be included in the MIS inventory.[2] The small-scale surveillance project is designed to provide gas generation and corrosion information of the MIS represented materials under worst-case moisture loadings. This information, in combination with material characterization, allows predictions of the behavior of 3013 packaged materials stored at DOE sites. Pressure, gas compositions, and corrosion were monitored in small scale reactors (SSRs) loaded with nominally 10 gram samples of plutonium bearing materials with nominally 0.5 weight percent (wt%) water, the upper limit allowed by the DOE's 3013 Standard.[1]

This report discusses sample MT1490 (SSR125) from the MIS Program inventory, a high-purity plutonium dioxide (PuO_2), with neptunium (Np), that originated in metal oxidation process at Plutonium Metallurgy R&D, Building 771, Room 182 at the Rocky Flats Plant, later known as the Rocky Flats Environment Technology Site (RFETS).[2]

MT1490 is representative of oxides generated from the following processes[2]:

- Process oxides from Pu metal and Pu/Np alloy oxidation at RFETS
- Oxides from Lawrence Livermore National Laboratory Pu metal burned at Savannah River Site (SRS)
- Metal oxidation at LANL of alloyed and unalloyed metal items from electrorefining, pyrochemical and other processes.

Figure 1. MT1490 upon arrival at LANL.

Material Characterization

The MT1490 as-received (AR) weapons grade plutonium oxide material is shown in Figure 1. After removing 100 g of material for testing, the remaining material was split into two approximately equal parts: one part was calcined at 800°C for 1 hour on February 16, 1999 and the other was calcined at 950°C for 2 hours on February 23, 1999. Several measurements of material characteristics that were obtained on the AR and calcined samples are summarized in Table 1. For sample loaded in the SSR, 7.9% AR, 46.6% calcined at 800°C and 45.4% calcined at 950°C were combined, and material characteristics for the loaded sample were calculated by weight-averaging the values for AR and calcined samples.

Table 1. Material Physical Characteristics for MT1490. Percentages show composition of sample loaded into SSR.

	AR (7.9%)	Calcined at 800 °C (46.6%)	Calcined at 950 °C (45.4%)	Estimated value for sample loaded into SSR
Specific Surface Area (SSA) 5-point (m^2 g^{-1})	3.56	0.8332	0.38*	0.84
Bulk Density (g cm^{-3})	5.536	6.014	6.150	
Tap Density (g cm^{-3})	6.920	7.334	7.500	
Pycnometer Density (g cm^{-3})	11.678	11.071	11.027	11.088

*Measured value of 0.0000 is unreasonable: estimated to be 54% of the value for the material calcined to 800°C which is consistent with the fit determined in Orr et al.[3]

Table 2 summarized the major non-actinide elemental constituents of the material. The plutonium facility's analytical chemistry group perfomed the analysis reported in Table 2a using calibrated procedures developed for characterization of plutonium oxide samples. Nitric acid dissolution can result in an undissolved residue which is not reported. Table 2a summarizes the wt% of key elements as well as any impurity present as 0.01 wt% or greater measured by atomic emission spectroscopy or mass spectroscopy. Table 2b lists the chloride and fluoride concentrations determined by ion chromatography. Oxygen is not measured and it is assumed to make up the difference between the sum of the listed elements plus actinides and 100%. No measurement of soluble species was conducted for this material.

Table 2. Elemental and isotopic data. Table 2a lists the wt% of major elemental constituents determined by atomic emission spectroscopy or mass spectroscopy. Table 2b lists wt% of chloride and fluoride determined by ion chromatography.

Table 2a.

Element	AR (wt%)	Calcined at 800 °C (wt%)	Calcined at 950 °C (wt%)
Aluminum	0.067	0.045	0.055
Barium	<0.001	0.002	0.015
Boron	0.012	0.009	0.010
Calcium	0.019	0.017	0.030
Carbon	0.051	0.011	0.013
Chromium	0.030	0.089	0.035
Copper	0.062	0.020	0.007
Gallium	0.051	0.043	0.041
Hydrogen	0.059	<0.005	<0.004
Iron	0.438	0.798	0.468
Magnesium	0.012	0.009	0.014
Nickel	0.017	0.049	0.019
Potassium	<0.004	0.006	0.023
Sodium	0.006	0.055	0.036

Table 2a. (continued)

Element	AR (wt%)	Calcined at 800 °C (wt%)	Calcined at 950 °C (wt%)
Strontium	<0.001	0.002	0.021
Sulfur	<0.003	0.004	0.032
Tantalum	0.010	0.006	0.009
Zirconium	0.054	0.032	0.051

Table 2b.

Ion	AR (wt%)	Calcined at 800 °C (wt%)	Calcined at 950 °C (wt%)
Chloride	0.008	0.088	0.017
Fluoride	0.005	0.019	0.010

Table 3 lists specific power measurements and isotopic data from calorimetry/gamma-ray spectrometry on as-received and combined samples (measurements on the combined sample were taken in 1999, 2001, and 2003). Specific power is reported in mW per gram of material, not per gram of Pu. The mass fraction of Pu (g of Pu/g of material) obtained for the combined sample in 1999 is much lower than the corresponding measurements for the same sample performed at other times. The reason for this discrepancy is unknown.

Table 3. Isotopic data, mass fraction of Pu and specific power for MT1490 on different measurement dates.

Isotope	As-received 6/5/1997 (g/g Pu)	Combined 3/10/1999 (g/g Pu)	Combined 11/26/2001 (g/g Pu)	Combined 11/25/2003 (g/g Pu)
Am-241	0.0022635	0.0023551	0.0018701	0.0019717
Np-237	0.00702379			0.00678102
Pu-238	0.0000935	0.0000947	0.0000502	0.0000639
Pu-239	0.9416884	0.9374329	0.9397107	0.9383315
Pu-240	0.0566345	0.0609585	0.0590331	0.0603433
Pu-241	0.0013336	0.0012639	0.0009559	0.0010113
Pu-242	0.0002500	0.0002500	0.0002500	0.0002500
Mass Fraction of Pu (g/g material)	0.85609	0.77463	0.87846	0.87184
Specific Power (mW/g material)	2.169	1.989	2.175	2.181

The expected specific power of MT1490 as a function of time from the 11/25/2003, the most recent specific power measurement date, are shown in Figure 2.

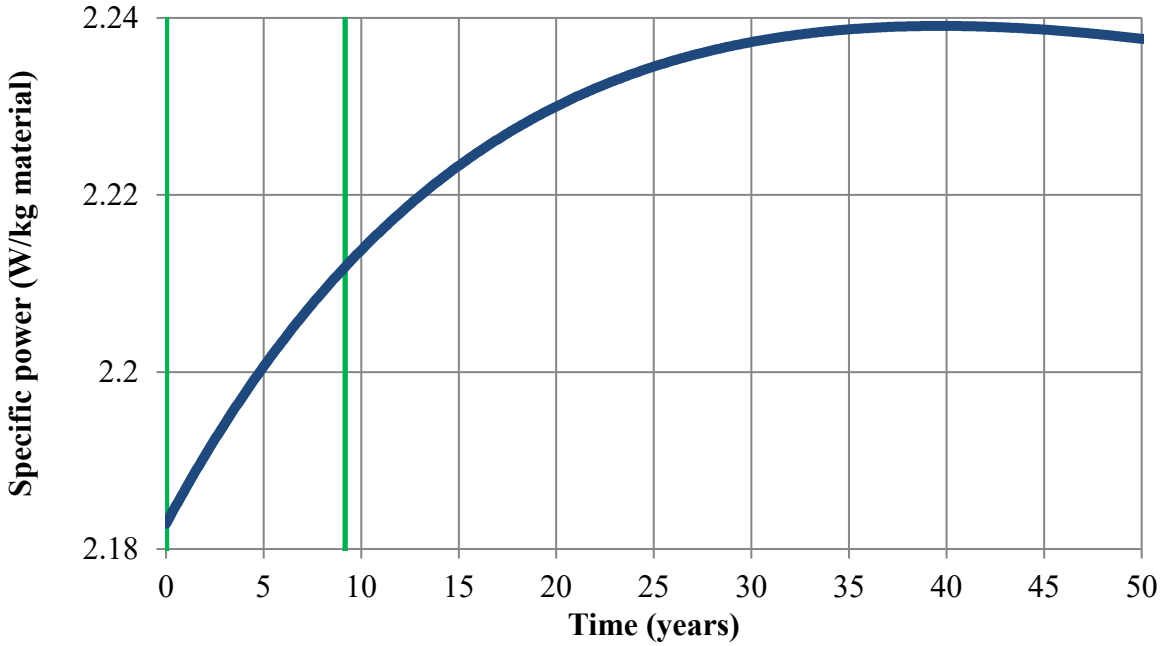

Figure 2. Expected specific power of MT1490 as a function of time from the last measurement date in 2003. The vertical green lines bind the time the sample was in the reactor.

Figure 3 provides information on He evolution as a function of time in MT1490.

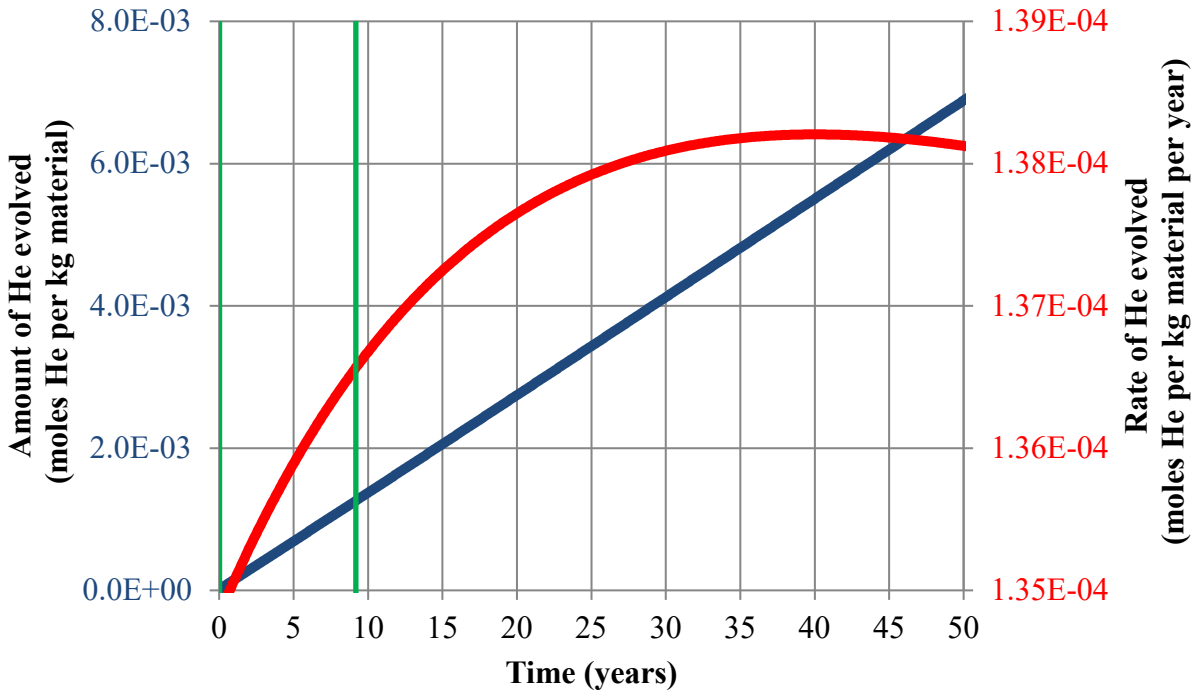

Figure 3. Amount of He evolved from alpha decay from MT1490 as a function of time (blue line) and the rate of He evolved as a function of time (red line). The vertical green lines bind the time the sample was in the reactor.

Experimental Procedure

The design of the small-scale reactor (SSR) system has been described previously.[4] The nominally 5 cm^3 internal volume of the SSR container is scaled to ~1/500th of the inner 3013 storage container. The SSR consists of a 304L stainless steel inner bucket, a container body welded to a Conflat flange, and a Conflat lid with tubing attachments for connections to a gas manifold and a low-internal-volume pressure transducer. The inner bucket is used to hold material and is inserted into the container body during loading activities. The inner bucket allows the fine plutonium oxide powder to be handled with minimal or no spillage. A low-internal-volume tubing connects the pressure transducer and manifold valves to the lid. Small-scale reactors have interchangeable parts with varying volumes. For this study, a Type H container with a total internal volume of 5.326 cm^3 was used.[5] A very small gas sampling volume of 0.05 cm^3 , contained between a pair of manifold sampling valves, allows gas composition to be determined with minimal effect on the internal gas pressure. A disassembled SSR is shown in Figure 4.

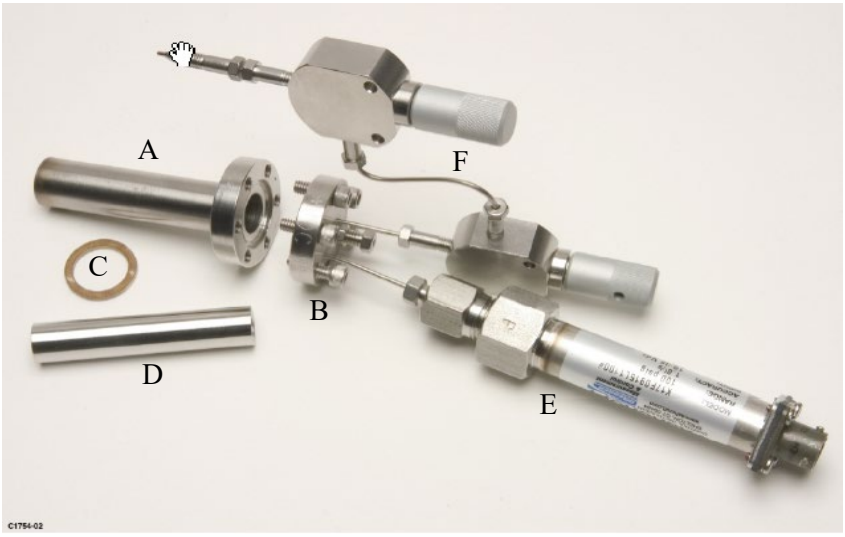

Figure 4. Dissassembled SSR: Conflat container body and flange (A), mating Conflat lid (B), copper gasket (C), inner bucket (D), pressure transducer (E), and a sampling volume between two sampling valves with connection to the gas manifold (F). Inner bucket slides into container body and holds the material.

Gas generation is to be characterized for each MIS represented material at the bounding moisture content of 0.5 wt%, where possible. The procedure to achieve 0.5 wt% moisture included (1) estimating the moisture content of the material as it was split for small-scale loading and (2) adding sufficient water to bring the total to 0.5 wt%. The moisture content of the material was estimated by weight loss upon heating to 200°C (LOI-200°C) of a 0.3 gram sample that was split from the parent material at the same time as the 10 g small-scale sample. The LOI-200°C sample was placed in a glass vial which remained in the glove box line with the small-scale sample until the LOI-200°C measurement was performed, typically one day or less after the sample split and just prior to SSR loading. LOI-200°C involved heating the 0.3 gram sample for 2 hours at 200°C, cooling the sample for 10 minutes and determining the mass difference of the material before

and after heating. The mass loss observed was attributed to adsorbed water. It was assumed that the LOI-200°C material contained an additional around 1.5 monolayer equivalent of water, approximately 0.05 wt%, as hydroxyls or chemically adsorbed water which was not removed by heating to 200°C.[4] The amount of water to be added to achieve 0.5 wt% total moisture was calculated as the difference between 0.5 wt% and the sum of the adsorbed water determined by LOI-200°C and the chemically adsorbed water assumed to be 0.05 wt%. In addition, a sample from the parent was split and placed in a glass vial inside of a hermetically sealed container. The water content of this sample was determined by Thermal Gravimetric Analysis-Mass Spectroscopy (TGA-MS). TGA-MS is inherently more accurate than LOI-200°C, although there can be errors associated with this method due to handling and excessive times before the sample is run. The TGA-MS results were not available at the time of loading and so could not be used to determine how much water to add to achieve 0.5 wt%.

To add moisture, a 10 gram sample of the MT1490 material was placed on a balance in a humidified chamber. Weight gain was recorded as a function of time. The sample was then placed into a small scale reactor. The glove boxes used for loading and surveillance were flushed with He, resulting in a glove box atmosphere of mainly He with a small amount of air. Some moisture loss was expected during transfer from the humidified chamber into the SSR in the very dry glove box atmosphere (relative humidity < 0.1 %). Transfer time from the balance where the final mass measurement was made to when the SSR was sealed was kept to approximately 45 seconds. The average weight loss during transfer for high purity oxides that had been equilibrated with high relative was measured to be 0.07 wt% per minute.[5] Therefore 0.05% was assumed to have been lost during the 45 seconds of loading when estimating total moisture content at loading.

The sealed SSR was placed in a heated sample array maintained at 55°C and monitored for approximately nine years. The SSR pressure and array temperature were recorded every fifteen minutes. The pressure data were reduced to weekly average values reported here. Gas composition was sampled at least annually. Fifty microliter gas samples were extracted through a gas mainfold. Fifty microliters corresponds to 1.1% of the free gas volume. The pressure drop on taking one of the gas samples was also 1.1%. The gas sample was analyzed using an Agilent 5890 GC (gas chromatograph) calibrated for He, H_2, N_2, O_2, CO_2, CO and N_2O. Water vapor was not measured in these samples.

At the termination of the experiment, a final GC gas sample was taken, and the SSR was removed from the array and allowed to cool to glove box temperature. Seven days later, the SSR lid was removed and a new lid containing a relative humidity sensor was placed on the container. After allowing an hour for the system to equilibrate, the relative humidity and temperature in the container were measured using a Vaisala HMT330 sensor and readout. The material was then removed from the container, and the moisture content in the material was measured by performing LOI-200°C.

Results

Loading

A 10 gram sample split from the parent was selected for loading into the SSR. The mass of the sample prior to moisture loading, $m_{mat,}$ the volume the material occupies calculated from m_{mat} and the pycnometer density, V_{mat}, and the calculated free gas volume within the SSR, V_{gas}, during the gas generation study are given in Table 4.

Table 4. Mass of sample and results of calculation of free gas volume for MT1490 using approach in *Obtaining G-values and rate constants from MIS data,* Appendix A.[5]

Mass of sample m_{mat}	**Volume of Material V_{mat}**	**Volume of SSR V_{SSR}**	**Free Gas Volume in SSR V_{gas}**
9.99 g	0.901 cm^3	5.326 cm^3	4.425 cm^3

TGA-MS Results

The sample split from the parent material for TGA-MS analysis was large enough to split into three subsamples. TGA trace and MS traces for channels that were above background for one of the three samples are shown in Figure 5.

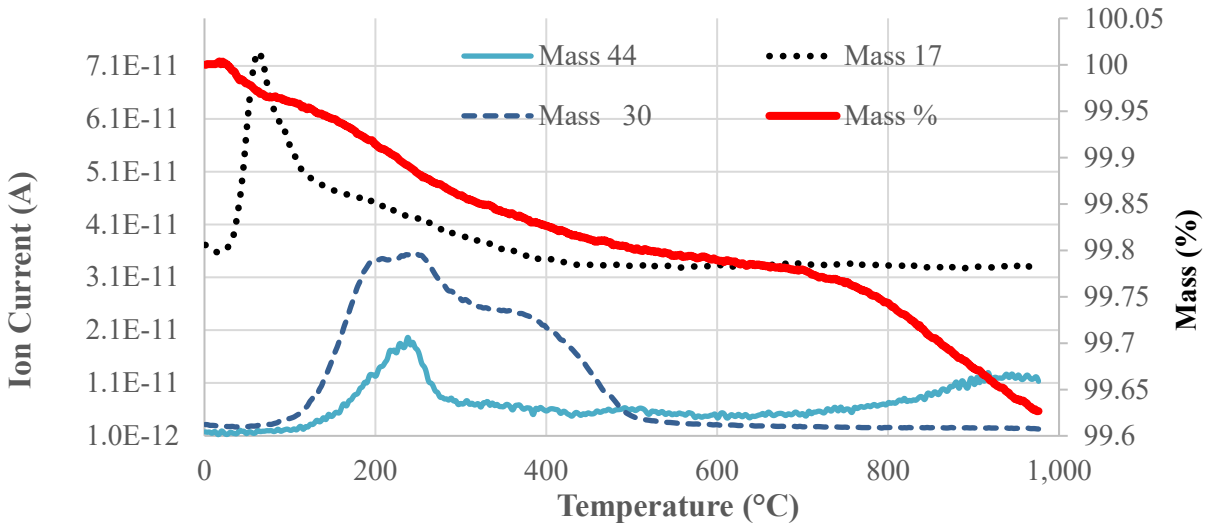

Figure 5. TGA-MS data for the MT1490 parent material. Mass 44.00 is CO_2, mass 30 is NO and mass 17 is H_2O.

Total initial moisture content in the loaded sample was determined by TGA-MS to be 0.057 wt%. Nitrogen oxides were the primary volatiles below 400°C. During the TGA-MS analysis, 0.05 wt% carbon dioxide and 0.09 wt% nitrogen dioxide was released. The LOI-200°C loss of 0.036 wt% underestimates the amount of water for this high-purity plutonium dioixde material.

Moisture addition

The measurements and assumptions used to estimate the true total moisture content at the time of loading are summarized in Table 5. The best estimate for the moisture content at loading is 0.40 wt% as given in Table 5 line 11, Estimated Total Moisture in loaded sample (using TGA-MS).

Table 5. Moisture data summary at loading.

	Parameter	SSR125	Units
1	Original Calcination Date	2/19/1999 2/23/1999	
2	Loading Date	12/4/2003	
3	Unloading Date	1/29/2013	
4	Initial sample weight (m_{mat})	9.99	g
5	Initial Moisture (Total) by TGA-MS	0.057	wt%
6	Initial Moisture (Weakly bound) by LOI-200 °C	0.036	wt%
7	Total Moisture added	0.39	wt%
8	Relative Humidity in glove box during loading (Data on temperature is not available)	0.1/--	% / °C
9	Estimated moisture loss during loading	0.05	wt%
10	Estimated **Weakly Bound Moisture** in loaded sample (using LOI) = Line 6 +Line7 –Line 9	0.38	wt%
11	Estimated **Total Moisture** in loaded sample (using TGA-MS) = Line 5 + Line 7 –Line 9	0.40	wt%

The moisture uptake as a function of exposure time to a high humidity atmosphere is plotted in Figure 6. The increase in mass is attributed to water adsorption by the material. When sample was left overnight in the humidified chamber, it adsorbed moisture above the target level. The dip in the moisture uptake curve between 17 and 18 hour reflects the fact that the sample was exposed to a reduced humidity to lower the moisture content before reaching the desired moisture uptake.

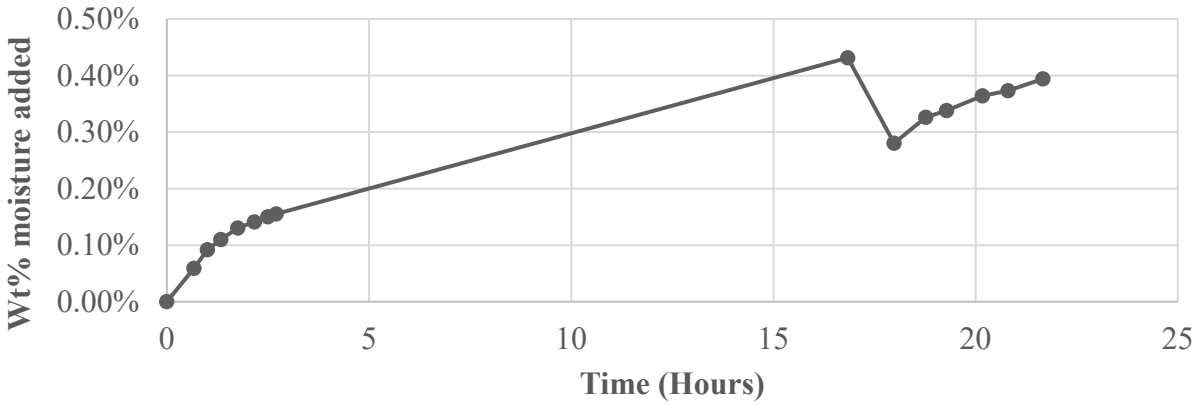

Figure 6. Moisture Addition Curve for MT1490

Gas Generation

The total pressure in SSR125 as a function of time, as well as the partial pressure of several gasses, is shown in Figure 7. Pressures reflect changes in the gasses in the reactor as well the 1.1% pressure drop due to each gas sampling event. In addition, the vapor pressure of water contributes an estimated 4 kPa to the total pressure, i.e., the sum of the partial pressures plotted and 4 kPa for water equals the total pressure. Note that the total pressure increase is less than the partial pressure increases from generated gases mainly due to loss of He partial pressure from sampling. Detailed information on gas composition and uncertainties is in Appendix 1 and on pressure in Appendix 2.

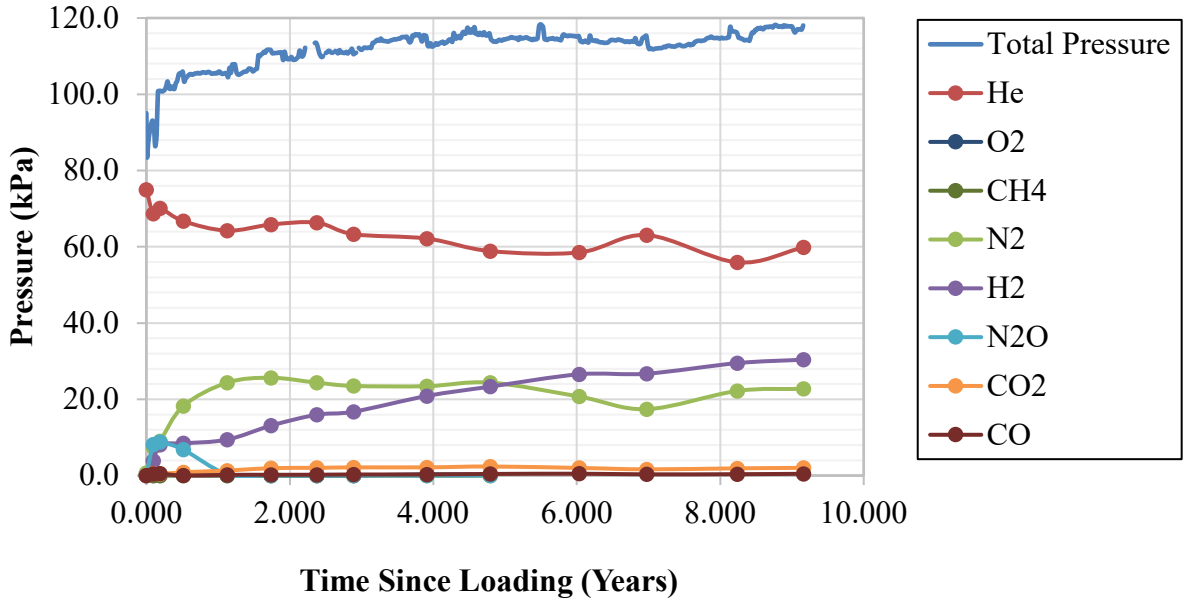

Figure 7. Total pressure and partial pressure of gases measured using a gas chromatograph as a function of time.

The initial pressure of 95 kPa dropped immediately to 84kPa, increased rapidly to 105 kPa in the first six months and gradually increased to a maximum pressure of 118 kPa over the next 9 years. Hydrogen increased to 4 kPa in the first month then gradually increased to the maximum measured pressure of 30 kPa over the next 9 years. Oxygen was a minor component in the headspace gas reaching a maximum of 0.3 kPa.

The net increase in total pressure during the experiment was primarily due to the generation of nitrogen as well as the hydrogen. Nitrogen increased rapidly to 7 kPa in the first month then then gradually increased to the maximum measured pressure of 26 kPa after 1.7 years and remained relatively constant over the next 7.5 years. Nitrous oxide pressure rose to 8 kPa in 35 days reaching a maximum of 9 kPa at 69 days before quickly reducing to undetectible levels where it remained for the rest of the experiment. Carbon dioxide rose to 2 kPa in the 1.5 years and remained relatively constant for the remainder of the experiment.

Moisture measurements on unloading

SSR125 was removed from the heated array and placed in a holder to cool. The relative humidity and temperature in the container were measured using a Vaisala HMT330 sensor and readout. No details are available for the time taken to complete the measurements. The weight loss in the material at termination by LOI-200°C was 0.15 wt%. Estimating that there was an additional 1.5 ML or 0.028 wt% strongly bound moisture, the total moisture at unloading based on LOI is 0.18 wt%.

The relative humidity in the reactor at unloading was 39.4%. Given this relative humidity, BET theory predicts approximately 1.35 monolayers (ML) or 0.025 wt% weakly bound water in the reactor (Appendix 4). Estimating that there was an additional 1.5 ML or 0.028 wt% strongly bound moisture, the total moisture at unloading based on RH is 0.053 wt%.

The unloading moisture data indicate a reduction of approximately 0.22 wt% (LOI) or 0.35 wt% (RH) or 50% - 90% of the moisture during the experiment. A similar large reduction in moisture was observed in previous reactors and is due, in part, to water condensing in the colder region of the reactor plumbing.[6]

Sample unloading and moisture data are summarized in Table 6.

Table 6. Unloading moisture data summary

	Parameter	Value	Units
1	Unloading moisture by LOI-200 °C	0.15	wt%
2	Estimated additional strongly bound moisture of 1.5 ML	0.028	wt%
3	Estimated **total moisture** at unloading from LOI = Line 1 + Line 2	0.18	wt%
4	Relative Humidity/Temperature in headspace at unloading	39.4 / 25.7	%/ °C
5	Number of monolayers at unloading RH and temperature using Figure A-1 and c=7.	1.35	ML
6	Mass of weakly bound water (RH) using # of MLs in line 5.	0.025	wt%
7	Estimated **total moisture** at unloading from RH = line 2 + line 6	0.053	wt%

Corrosion

Images of the inner buckets of SSR125 are shown in Figure 8. No images of the bottom of the bucket were available.

a) 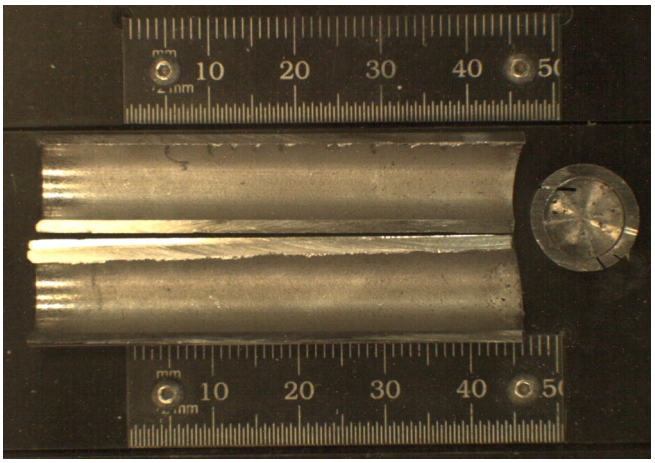

b) 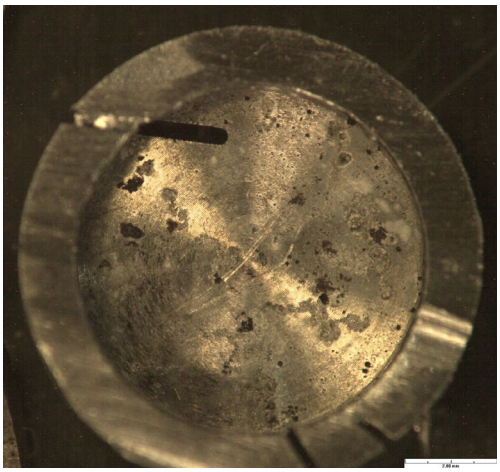

c) 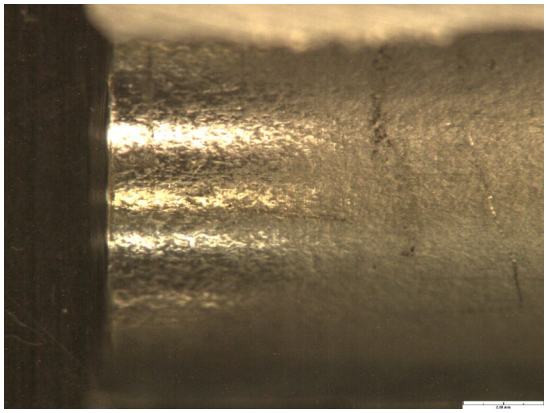

d) 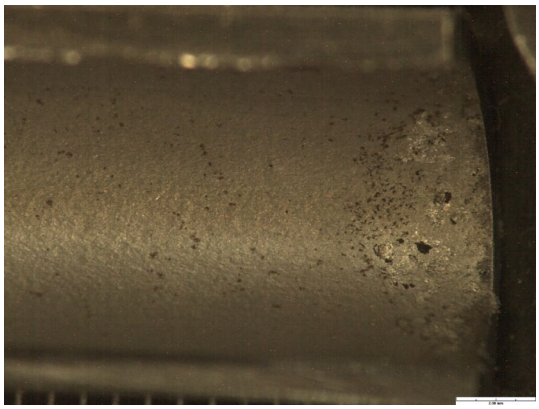

e) 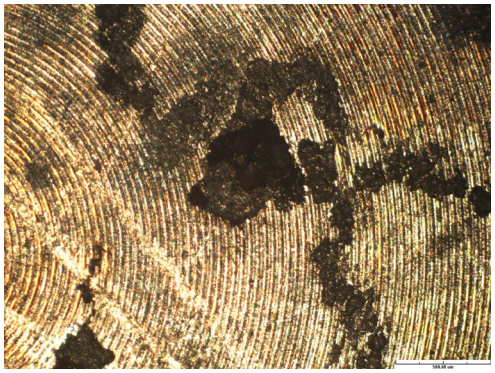

Figure 8. a) inner bucket b) bottom of inner bucket c) close up inner bucket wall in the headspace d) close up of the contact region of the inner bucket wall near the bottom e) close up of suspect corrosion/pitting on bottom of inner bucket

Limited corrosion was observed in the inner bucket with a clear distinction between the shinier headspace and the material region. Suspect small pits were observed in the bottom section which was not expected in this low chloride material. Additional photos of bottom of the inner bucket are in Appendix 3.

Discussion

A goal of the small-scale surveillance studies is to understand the hydrogen gas generation response of material exposed to moisture over a broad range of materials. Hydrogen partial pressure curves can be analyzed to obtain hydrogen G-values and formation and consumption rate constants assuming that the hydrogen gas is formed either from radiolysis or from surface decomposition of water.[7] In order to perform these calculations knowledge of the moisture content of the material during the study and the radiation dose to the moisture is required. We will first discuss the amount of moisture on the material during the study and use the results as input to the $G(H_2)$ and rate constant calculations. We will follow those results with a discussion of the observation of other gases.

Unlike plutonium-bearing materials currently stored in 3013 containers throughout the DOE complex, MT1490 was exposed to the glove box environment for nearly five years after calcination prior to loading. A significant formation of hydroxyls on the oxide surface is expected after this much time. Gases, such as NOx and CO_2, would also be adsorbed to the surface as indicated in the TGA-MS, Figure 5. The presence of these species may alter the gas generation behavior compared with recently calcined plutonium oxide.

The H_2 G-value and rate constants

It is recommended that $G(H_2)$ and rate constants be calcuated for materials where H_2 is observed. The mathematical formalism is given in *Obtaining G-values and rate constants from MIS data*.[7] The formation rate constant, k_1, has been redefined in this report. The hydrogen gas generation rate was determined by fitting the hydrogen partial pressure data to Equation 1 which expresses H_2 pressure as a function of time (Figure 9).

$$p = a\left(1 - e^{-bt}\right) = A_0\, k_1/k_2 \left(1 - e^{-k2t}\right) = \mathbf{Pmax}\left(1 - e^{-k2t}\right) \qquad \text{Equation 1}$$

where A_0 , the initial active water, has units of kPa, and k_1, the H_2 formation rate constant and k_2 , the H_2 consumption rate constant, have units of day^{-1}.

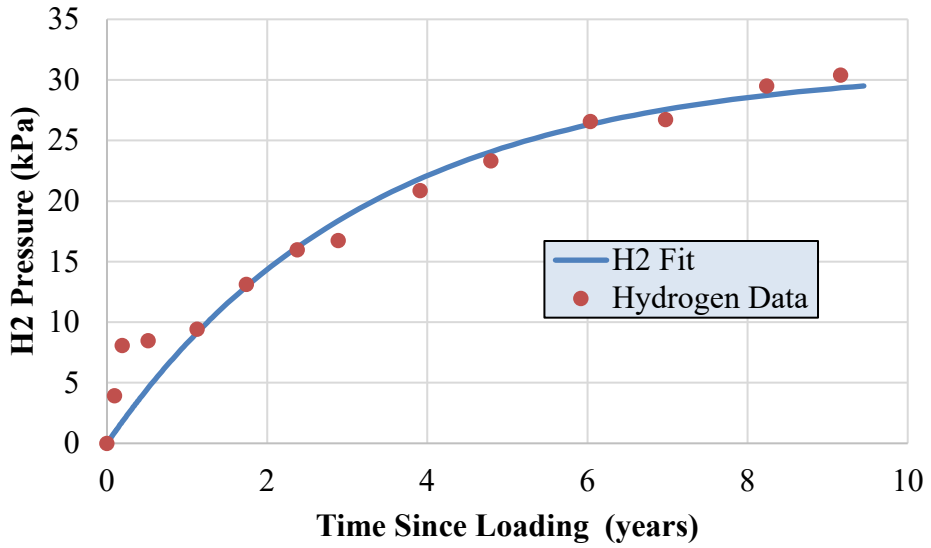

Figure 9. The hydrogen partial pressure and the fit to Equation 1, or zeroth order (constant) formation and first order consumption reaction.

The values for the fit parameters yielding the curve in Figure 9 are given in Table 7. We will use these values to calculate $G(H_2)$ and the rate of the hydrogen consumption reactions.

Table 7. The fit parameters and standard errors from the hydrogen generation data

Small-scale Surveillance sample identification	$a = A_0 k_1/k_2 = P_{max}$	$b = k_2$	A_0k_1 **(rate of hydrogen formation)**
SSR125	31.2 kPa	0.00084 day^{-1}	0.026 kPa/day 7.6 x 10^{-6} wt%/day
Standard Error	2.5	.00016	

This derivation assumes that there is no appreciable decrease in the amount of active water in the system. To evaluate the more complex situation with water depletion, a more complex set of rate equations is needed. However, the moles of water consumed can be approximated as being equal to the hydrogen formation rate, A_0k_1 (0.026 kPa/day) multiplied by the time the reactor was loaded (3344 days), 87 kPa, 0.0025g or 0.025 wt%. Assuming the initial water in the reactor was 0.40 wt% (TGA at loading), this represents a 6% reduction in the total amount of water between the beginning and the end of the experiment. Alternatively, assuming the initial active water is the sum of the 0.025 wt% weakly bound water at unloading from RH and the 0.025 wt% water consumed to form hydrogen based on the fit, 0.05 wt%, 50% of the weakly bound water reacted over the course of the experiment. A plot of the estimated wt% water active in hydrogen formation, A(t) remaining in the system as a function of time, t, is plotted in Figure 10 using the Equation 2 below, assuming the initial active water was 0.05 wt%.

$$A(t) = A_0 - A_0 k_1 t = 0.05 \text{ wt\%} - 7.6 \times 10^{-6} \text{ wt\%/day} * t(\text{days}) \quad \text{Equation 2}$$

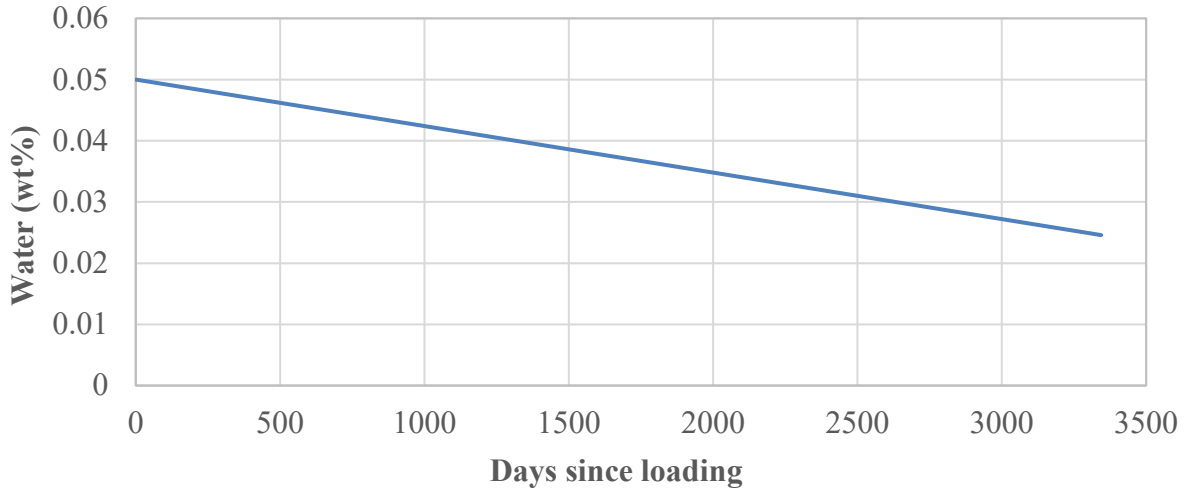

Figure 10. Graph of the estimated active water, A(t), in SSR125 as a function of time, where A_0 is expressed in terms of wt% of water.

Estimation of the amount of moisture on the material during the gas generation study

Moisture adsorbed on high-purity plutonium dioxide such as MT1490 is thought to exist as physisorbed (weakly bound) water that behaves according to BET theory[8] and as chemisorbed (strongly bound) water with very low chemical activity (very low water vapor pressure). The latter water can be described as surface hydroxyls and is removed from the plutonium dioxide surface only at high temperatures. In order to use BET theory to estimate the amount of physisorbed and chemisorbed water on the material during the experiment, the SSA, the amount of water in a monolayer, and the RH are needed. RH data was only available at the termination of the experiment.

The difference between the best estimate of the amount of water in SSR125 when the material was loaded (0.040 g from TGA) and unloaded (0.0025 g from RH), 0.0375 g, is much greater than the amount of water that produced H_2 (0.009 g) plus the amount of water that would be in the gas phase at unloading, 0.00004 g. A gradual conversion of physisorbed water to chemisorbed water (hydroxyls) during the experiment would contribute to lower measured moisture content at the termination of the experiment but this is expected to be less than 1.0 monolayers (0.002 g) of water.[9, 10]

The additional difference is probably due to water condensing in the colder region of the reactor plumbing.[10] During the gas generation study, the condensed moisture in the cold region of the plumbing is located at a sufficient distance from the material that the radiation dose it receives is orders of magnitude smaller than the radiation dose the water associated with the material receives. This water is NOT expected to contribute to gas generation and would result in a low value for G(H2) in G-value calculations.

Moisture at loading (TGA) overestimates the water receiving radiation dose resulting in gas generation since it includes water condensed on the cold region of the reactor. Moisture estimates that include the 1.5 ML of chemisorbed water may also overestimate water involved in gas generation since it is unlikely the strongly bound water participates. Table 8 summarizes the amount of water on the material, in the gas phase, and decomposed to form H_2 expressed as weight percent, moles, grams, and monolayers.

Table 8. The amount of water adsorbed on the material, in the gas phase, and decomposed to form H_2 expressed as moles, grams, and monolayers. Calculations use SSA = 0.84 m^2 g^{-1} , m_{mat} = 9.99 g and V_{gas} = 4.425 cm^3. The amount of strongly bound chemisorbed water on the material was assumed to be 1.5 monolayers wt% at all times.

Water Source	**Amount of Water**			
	wt%	g	moles	monolayers
	0.0185	0.00185	0.00017	1
Estimated Total moisture at loading from Table 5	0.40	0.0400	0.0022	21.6
Water consumed to produce H_2 (from fit $A_0 k_1$ = 0.026 kPa/day)	0.025	0.0025	0.00014	1.4
Water vapor at unloading, 25.7 ºC and 39.4% RH (1.3 kPa)	0.0004 (equivalent)	4×10^{-5}	2×10^{-6}	0.02 (equivalent)
Chemisorbed water (1.5 ML)	0.028	0.0028	0.00015	1.5
On material at unloading by LOI	0.15	0.0150	0.0008	8.1
On material at unloading by RH	0.025	0.0025	0.00014	1.4
Total in system at loading from unloading LOI data = water consumed +water vapor + chemisorbed + LOI	0.20	0.020	0.00issu11	10.8
Total in system at loading from unloading RH data = water consumed +water vapor + chemisorbed + RH	0.078	0.0078	0.00043	4.2

(Note: Additional moisture could have been consumed in formation of the corrosion products such as iron hydroxide)

A_0, k_1, and k_2 are used to calculate $G(H_2)$ and the rate constants for the hydrogen formation and consumption surface reactions calculated from equations in Appendix 6. Because of the

uncertainty in determining the amount of water involved in the hydrogen generation, several values are used for the variable m_{H2O} for comparison The stopping power ratio for MT1490 material, $\frac{S_{H_2O}}{S_{mat}}$, is 3.7 (Appendix 5). Results for the multiple choices of water, using equations from Appendix 6, are reported in Table 9 and Table 10.

Table 9. G(H_2) calculated from the reaction parameters and the estimated moisture content using equation A6-4 in Appendix 6 assuming radiolytic decomposition of water to form H_2.

Water Source	$\mathbf{m_{H2O}}$	***G(H₂)*** molecules $100eV^{-1}$
Estimated Total Moisture at Loading from Table 5	0.040 g	0.015
Water consumed to produce H_2 OR On material at unloading by RH	0.0025	0.24
LOI at unloading	0.015g	0.04
RH at unloading	0.0025 g	0.24
Total moisture at loading from unloading LOI data	0.02g	0.03
Total moisture at loading from unloading RH data	0.0078 g	0.076

Table 10. Rate constants calculated from the reaction parameters and the estimated moisture content from the fit (A_0) assuming surface catalyzed decomposition of water to form H_2.

Variable	**Equation in Appendix 6**	**Value**	**Units**
k_1	A6-5	2.9E+11	molecules s^{-1}
k_2	A6-6	9.5E+9	molecules s^{-1} kPa^{-1}
R_{for}	A6-8	0.21	nanomoles m^{-2} hr^{-1}
R_{con}	A6-9	0.0068	nanomoles m^{-2} hr^{-1} kPa^{-1}

Figure 11 illustrates the large differences in G(H_2) depending on the choice of water and compares the G(H_2) values determined in this study with those reported previously.[11]

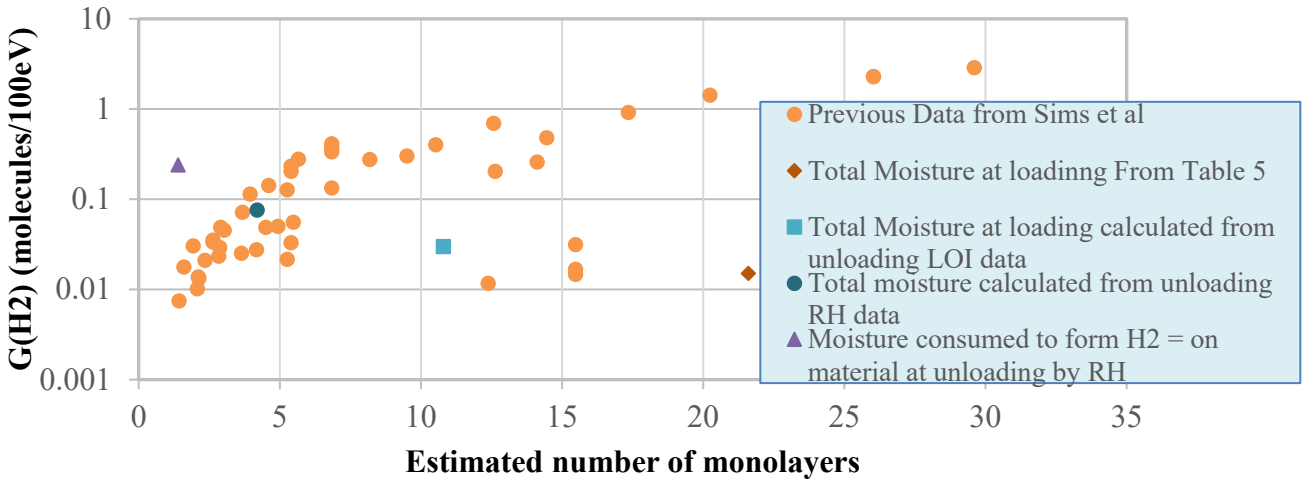

Figure 11. Comparison of calculated $G(H_2)$ plotted against the number of calculated water monolayers determined in this study with those from previous research.

Behavior of N_2 and NO_X gases

The nitrogen dioxide detected by TGA-MS on the 10 g sample at loading are a possible source for the N_2 and N_2O observed in the gas phase. (The compounds actually bound to plutonium dioxide surface could have been any of the general form NOx). The number of moles of nitrogen gas and nitrous oxide present in the head space at the maximum and at the termination of the experiment were calculated using the ideal gas law, n = PV/RT, where V = 4.425 cm^3, T = 328 K, and P = partial pressure of the gas (P_{N2}=22.8 kPa at termination and 25.7 kPa at maximum detected, P_{N2O} = 0 kPa at termination and 8.8 kPa a maximum, P_{CO2}= 2.0 kPa at termination and 2.4 kPa a maximum). Results are summarized in Table 11.

Table 11. The amount of carbon and nitrogen species detected on the surface (TGA) compared to the amount detected in the gas phase.

	CO_2 (moles)	**NO_2 (moles)**	**N_2 (moles)**	**N_2O**	**N (moles)**
Sample (Loading-TGA-MS)	1.1×10^{-4}	2.0×10^{-4}	Not measured	Not measured	2.0×10^{-4}
Head Space (Termination-GC)	3.9×10^{-6}	Not measured	3.7×10^{-5}	0	7.4×10^{-5}
Max Detected in Head Space over duration of experiment (GC)	3.2×10^{-6}	Not measured	4.1×10^{-5}	1.4×10^{-5}	1.1×10^{-4}

Approximately 3% of the carbon dioxide detected by TGA-MS in the sample before loading was released into the headspace during the experiment. Approximately 55% of the

nitrogen in the NOx gases detected by TGA-MS before loading was released from the surface as N_2 or N_2O by the termination of the experiment. Prior to loading the sample in the small scale reactor, the plutonium dioxide powder was exposed to air for nearly five years (nitrogen and oxygen with small amounts of water and carbon dioxide). The sample was placed in a helium atmosphere within the small scale reactor with a large partial pressure of water. A possible explantion for the increase in CO_2 , N_2 and to a lesser extent N_2O, is that the water displaced chemically adsorbed CO_2 from the surface sites.

Behavior of He

The alpha decay of the Pu and Am creates He, which may escape the oxide into the gas phase. The amount of He created depends upon the mass of the material and the rate of decay of the various isotopes. The rate of decay can be illustrated graphically as the specific wattage calculated from the reported isotopics, Figure 2. Results were calculated using the last reported isotopics measurements taken on November 25, 2003 that are reported in Table 3. The integrated and differential amount of He evolved as a function of time are shown in Figure 3.

The amount of He created due to alpha decay over the 9.2 years the material was in the SSR is estimated to be 1.3×10^{-5} moles for the 10 g sample. This amount of He would result in a gas pressure increase of 7.8 kPa in the 4.425 ml of gas volume and gas temperature of 328 K, if all the He was released into the gas phase. Instead, the He pressure declined by approximately 15 kPa, which is 5.1 kPa more than the expected 9.9 kPa decline due to the 14 gas samplings. Thus, it appears that there may have been a leak in the reactor of 5% or more of the headspace gas during the 9.2 years of the experiment. This analysis does not account for the large uncertainties associated with the He gas measurements.

Conclusions

The MIS item MT1490 was entered into surveillance in December, 2003, and removed from surveillance in January of 2013. The amount of water on the material during the gas generation study has an upper limit of 0.4 wt% and a lower lower limit of 0.0025 wt%. The gas generation was dominated by N_2 and H_2. Hydrogen was generated to a maximum partial pressure of 30.2 kPa at the termination of the experiment. The oxygen reached a maximum partial pressure of approximately 0.3 kPa. Corrosion was also observed in the material phase and pitting was observed in the bottom of the inner bucket.

Acknowledgements

Funding for this work was provided to the MIS Program by the Assistant Manager for Nuclear Materials Stabilization, Savannah River Operations Office, Department of Energy's Office of Environmental Management..

References

1. U. S. Department of Energy, Stabilization, Packaging, and Storage of Plutonium-Bearing Materials. U.S. Department of Energy: Washingon, D.C., 2018.
2. Narlesky, J. E.; Peppers, L. G.; Friday, G. P. *Complex-Wide Representation of Material Packaged in 3013 Containers*; LA-UR-14396; Los Alamos National Laboratory: Los Alamos, NM, 2009.
3. Orr, R. M.; Sims, H. E.; Taylor, R. J., A review of plutonium oxalate decomposition reactions and effects of decomposition temperature on the surface area of the plutonium dioxide product. *Journal of Nuclear Materials* **2015,** *465*, 756-773.
4. Veirs, D. K.; Berg, J. M.; Crowder, M. L. *The effect of plutonium dioxide water surface coverage on the generation of hydrogen and oxygen*; LA-UR-12-22377; Los Alamos National Laboratory: Los Alamos, NM, 2012.
5. Worl, L., Berg, John, Bielinberg, Patricia, Carrillo, Alex, Martinez, Max, Montoya, Adam, Veirs, Kirk, Puglisi, Charles, Rademacher, Dave, Schwartz, Dan, Harradine, David, McInroy, Rhonda, Hill, Dallas, Prenger, Coyne, Steward, Jim *Shelf Life Surveillance for PuO2 Bearing Materials FY04 Second Quarterly Report*; Los Alamos National Laboratory: 2004.
6. Veirs, D. K., Stroud, M.A., Berg, J., Narlesky, J. Worl, L., Martinez, M.,. Carillo, A. *MIS High-Purity Plutonium Oxide Metal Oxidation PRoduct TS707001 (SSR123): Final Report*; LA-UR-17-27172; Los Alamos National Laboratory: Losa Alamos, NM, 2017.
7. Veirs, D. K.; Berg, J. M.; Stroud, M. A. *Obtaining G-values and rate constants from MIS data*; LA-UR-17-23787; Los Alamos National Laboratory: Los Alamos, NM, 2017.
8. Brunauer, S.; Emmett, P. H.; Teller, E., Adsorption of Gases in Multimolecular Layers. *Journal of the American Chemical Society* **1938,** *60*.
9. Veirs, D. K.; Berg, J. M.; Hill, D. D.; Harradine, D. M.; Narlesky, J. E.; Romero, E. L.; Trujillo, L.; Wilson, K. V. *Water radiolysis on plutonium dioxide: Initial results identifying a threshold relative humidity for oxygen gas generation*; LA-UR-12-26423; Los Alamos National Laboratory: Los Alamos, NM, 2012.
10. Veirs, D. K. S., M. A.; Martinez, M. ; Carrillo, A.; Berg, J.; Narlesky, J.; Worl, L. *MIS High-Purity Plutonium Oxide Metal Oxidation Product TS707001 (SSR123): Final Report*; LA-UR-17-27172; Los Alamos National Laboratory: Los Alamos, NM, 2017.
11. Sims, H. E. W., K. J.; Brown, J.; Morris, D.; Taylor, R. J., Hydrogen yields from water on the surface of plutonium dioxide. *Journal of Nuclear Materials* **2013,** (437), 359-364.
12. Haschke, J. M.; Ricketts, T. E., Adsorption of water on plutonium dioxide. *Journal of Alloys and Compounds* **1997,** *252*, 148-156.
13. (a) Haschke, J. M.; Allen, T. H.; Morales, L. A., Reaction of Plutonium Dioxide with Water: Formation and Properties of PuO_{2+x}. *Science* **2000,** *287*, 285-286; (b) Haschke, J. M.; Allen, T. H.; Morales, L. A., Reactions of plutonium dioxide with water and hydrogen–oxygen mixtures: Mechanisms for corrosion of uranium and plutonium. *Journal of Alloys and Compounds* **2001,** *314*, 78-91.

Appendix 1: Gas Generation Partial Pressure Data and Uncertainties in kPa

Note: Total pressure values used to determine partial pressures were reduced by 4kPa to correct for the estimated partial pressure of water vapor. Partial pressures were corrected for variation in the sensitivity of the GC with time. The average manifold background pressure was subtracted from the partial pressures.

Date	**12/4/03**	**1/8/04**	**2/11/04**	**6/9/04**	**1/18/05**	**8/30/05**	**4/19/06**	**10/23/06**	**10/31/07**	**9/18/08**	**12/15/09**	**11/23/10**	**2/27/12**	**1/29/13**
Days	0	35	69	188	411	635	867	1054	1427	1750	2203	2546	3007	3344
CO_2	0.0	0.5	0.4	0.9	1.3	1.9	2.0	2.2	2.2	2.4	2.0	1.6	1.9	2.0
N_2O	0.0	8.1	8.8	6.8	0.4	0.0	0.0	0.0	0.0	0.0	0.0	0.0	0.0	0.0
He	75.0	68.7	70.1	66.7	64.2	65.8	66.3	63.3	62.2	58.9	58.5	63.1	55.9	59.9
H_2	0.0	3.9	8.1	8.5	9.4	13.1	16.0	16.7	20.9	23.3	26.6	26.7	29.5	30.4
O_2	0.2	0.0	0.0	0.1	0.0	0.0	0.1	0.0	0.3	0.3	0.3	0.1	0.0	0.1
N_2	0.7	7.4	9.0	18.2	24.4	25.7	24.4	23.5	23.4	24.4	20.7	17.4	22.2	22.8
CH_4	0.0	0.0	0.0	0.0	0.0	0.0	0.0	0.0	0.0	0.0	0.0	0.0	0.0	0.0
CO	0.0	0.4	0.5	0.0	0.2	0.2	0.2	0.3	0.3	0.4	0.5	0.3	0.4	0.5
H_2O (estimate)	4.0	4.0	4.0	4.0	4.0	4.0	4.0	4.0	4.0	4.0	4.0	4.0	4.0	4.0
SUM check	80.0	93.1	101.0	105.2	103.9	110.8	113.0	110.0	113.3	113.7	112.6	113.3	113.9	119.6

Appendix 1: Gas Generation Partial Pressure Data and Uncertainties in kPa (continued)

Note: The errors are determined from 1 σ uncertainties in the total pressure and 1 σ uncertainties in the GC sensitivities to the various gases which are determined during the calibration of the GC.

Date	**12/4/03**	**1/8/04**	**2/11/04**	**6/9/04**	**1/18/05**	**8/30/05**	**4/19/06**	**10/23/06**	**10/31/07**	**9/18/08**	**12/15/09**	**11/23/10**	**2/27/12**	**1/29/13**
Days	0	35	69	188	411	635	867	1054	1427	1750	2203	2546	3007	3344
CO_2	0.00	0.02	0.02	0.04	0.05	0.07	0.07	0.07	0.08	0.08	0.07	0.06	0.06	0.49
N_2O	0.00	0.19	0.21	0.17	0.02	0.01	0.00	0.00	0.01	0.01	0.00	0.00	0.00	0.00
He	1.55	1.42	1.44	1.38	1.33	1.36	1.37	1.31	1.28	1.22	1.21	1.30	1.30	0.08
H_2	0.00	0.08	0.17	0.18	0.20	0.28	0.34	0.35	0.44	0.49	0.55	0.56	0.56	0.02
O_2	0.02	0.00	0.00	0.01	0.00	0.00	0.01	0.01	0.02	0.02	0.02	0.01	0.01	0.03
N_2	0.03	0.17	0.21	0.40	0.53	0.56	0.53	0.51	0.52	0.54	0.46	0.39	0.39	0.03
CH_4	0.00	0.00	0.00	0.00	0.00	0.00	0.00	0.00	0.00	0.00	0.00	0.00	0.00	0.00
CO	0.00	0.02	0.02	0.00	0.02	0.02	0.02	0.02	0.02	0.03	0.03	0.02	0.02	0.12

Appendix 2: Gas Generation: Total Pressure

Date	Pressure (kPa)	Date	Pressure (kPa)	Date	Pressure (kPa)	Date	Pressure (kPa)	Date	Pressure (kPa)
12/5/2003	95.0	6/21/2004	104.0	1/10/2005	105.6	8/1/2005	110.9	2/20/2006	112.2
12/8/2003	83.6	6/28/2004	104.5	1/17/2005	105.4	8/8/2005	111.6	2/27/2006	
12/15/2003	87.6	7/5/2004	104.9	1/24/2005	104.5	8/15/2005	111.7	3/6/2006	
12/22/2003	90.2	7/12/2004	105.2	1/31/2005	106.9	8/22/2005	111.7	3/13/2006	
12/29/2003	92.1	7/19/2004	105.3	2/7/2005	105.6	8/29/2005	111.6	3/20/2006	
1/5/2004	93.1	7/26/2004	105.1	2/14/2005	107.8	9/5/2005	110.8	3/27/2006	
1/12/2004	92.3	8/2/2004	105.3	2/21/2005	107.7	9/12/2005	110.8	4/3/2006	
1/19/2004	86.4	8/9/2004	105.5	2/28/2005	107.8	9/19/2005	110.8	4/10/2006	113.5
1/26/2004	89.1	8/16/2004	105.5	3/7/2005	105.9	9/26/2005	110.8	4/17/2006	113.5
2/2/2004	100.7	8/23/2004	105.6	3/14/2005	105.2	10/3/2005	110.9	4/24/2006	112.6
2/9/2004	100.9	8/30/2004	105.5	3/21/2005	105.2	10/10/2005	111.0	5/1/2006	111.1
2/16/2004	100.9	9/6/2004	105.5	3/28/2005	105.3	10/17/2005	110.8	5/8/2006	110.2
2/23/2004	100.7	9/13/2004	105.7	4/4/2005	105.6	10/24/2005	110.9	5/15/2006	109.8
3/1/2004	100.9	9/20/2004	105.8	4/11/2005	105.8	10/31/2005	109.0	5/22/2006	110.0
3/8/2004	101.2	9/27/2004	105.7	4/18/2005	106.0	11/7/2005	111.1	5/29/2006	
3/15/2004	102.1	10/4/2004	105.6	4/25/2005	105.9	11/14/2005	109.9	6/5/2006	110.8
3/22/2004	103.4	10/11/2004	105.8	5/2/2005	106.2	11/21/2005	109.2	6/12/2006	111.1
3/29/2004	101.6	10/18/2004	105.9	5/9/2005	106.7	11/28/2005	109.3	6/19/2006	111.4
4/5/2004	101.4	10/25/2004	105.7	5/16/2005	106.7	12/5/2005	109.3	6/26/2006	111.3
4/12/2004	102.0	11/1/2004	105.4	5/23/2005	106.5	12/12/2005	109.8	7/3/2006	110.9
4/19/2004	101.5	11/8/2004	105.4	5/30/2005	106.0	12/19/2005	109.1	7/10/2006	110.9
4/26/2004	101.4	11/15/2004	105.5	6/6/2005	106.3	12/26/2005	109.1	7/17/2006	
5/3/2004	102.9	11/22/2004	105.6	6/13/2005	106.6	1/2/2006	109.1	7/24/2006	111.4
5/10/2004	103.5	11/29/2004	105.5	6/20/2005	106.8	1/9/2006	109.5	7/31/2006	111.0
5/17/2004	105.1	12/6/2004	105.9	6/27/2005	110.2	1/16/2006	109.9	8/7/2006	110.8
5/24/2004	105.5	12/13/2004	105.9	7/4/2005	110.0	1/23/2006	111.5	8/14/2006	111.6
5/31/2004	105.2	12/20/2004	105.5	7/11/2005	110.4	1/30/2006	110.1	8/21/2006	111.0
6/7/2004	105.9	12/27/2004	105.3	7/18/2005	110.7	2/6/2006	109.9	8/28/2006	111.0
6/14/2004	103.3	1/3/2005	105.4	7/25/2005	111.1	2/13/2006	110.5	9/4/2006	110.8

Appendix 2 Gas Generation: Total Pressure (continued)

Date	Pressure (kPa)	Date	Pressure (kPa)	Date	Pressure (kPa)	Date	Pressure (kPa)	Date	Pressure (kPa)
9/11/2006	110.9	3/26/2007	114.0	10/8/2007	113.9	4/21/2008	114.7	11/3/2008	114.3
9/18/2006	111.1	4/2/2007	113.9	10/15/2007	115.4	4/28/2008	115.8	11/10/2008	114.2
9/25/2006	110.7	4/9/2007	113.9	10/22/2007	115.4	5/5/2008	116.4	11/17/2008	114.1
10/2/2006	111.2	4/16/2007	113.8	10/29/2007	115.3	5/12/2008	115.9	11/24/2008	114.4
10/9/2006	111.2	4/23/2007	113.9	11/5/2007	112.8	5/19/2008	116.1	12/1/2008	114.4
10/16/2006	112.0	4/30/2007	114.1	11/12/2007	112.6	5/26/2008	117.5	12/8/2008	114.5
10/23/2006	110.6	5/7/2007	114.2	11/19/2007	113.4	6/2/2008	116.4	12/15/2008	114.6
10/30/2006	110.7	5/14/2007	114.3	11/26/2007	112.6	6/9/2008	116.2	12/22/2008	114.7
11/6/2006	110.9	5/21/2007	114.4	12/3/2007	112.6	6/16/2008	117.0	12/29/2008	114.8
11/13/2006		5/28/2007	114.4	12/10/2007	112.9	6/23/2008	116.2	1/5/2009	115.0
11/20/2006	112.2	6/4/2007	114.5	12/17/2007	113.4	6/30/2008	117.6	1/12/2009	114.8
11/27/2006	111.8	6/11/2007	114.6	12/24/2007	113.0	7/7/2008	115.9	1/19/2009	114.8
12/4/2006	111.6	6/18/2007	114.6	12/31/2007	113.2	7/14/2008	115.9	1/26/2009	114.7
12/11/2006	111.9	6/25/2007	115.0	1/7/2008	113.5	7/21/2008	115.6	2/2/2009	114.8
12/18/2006	112.2	7/2/2007	115.0	1/14/2008	113.5	7/28/2008	116.1	2/9/2009	114.2
12/25/2006	112.2	7/9/2007	115.0	1/21/2008	113.8	8/4/2008	115.8	2/16/2009	115.0
1/1/2007	112.1	7/16/2007	114.9	1/28/2008	113.3	8/11/2008	115.5	2/23/2009	114.6
1/8/2007	112.2	7/23/2007	115.1	2/4/2008	113.5	8/18/2008	116.3	3/2/2009	114.8
1/15/2007	112.2	7/30/2007	114.2	2/11/2008	113.6	8/25/2008	115.6	3/9/2009	114.7
1/22/2007	112.2	8/6/2007	113.6	2/18/2008	114.1	9/1/2008	115.4	3/16/2009	114.9
1/29/2007	113.4	8/13/2007	114.0	2/25/2008	114.4	9/8/2008	115.6	3/23/2009	114.9
2/5/2007	113.5	8/20/2007	115.4	3/3/2008	114.3	9/15/2008	116.0	3/30/2009	114.7
2/12/2007	113.8	8/27/2007	115.2	3/10/2008	113.8	9/22/2008	114.4	4/6/2009	114.5
2/19/2007	114.2	9/3/2007	115.7	3/17/2008	116.1	9/29/2008	114.1	4/13/2009	114.5
2/26/2007	114.2	9/10/2007	115.7	3/24/2008	114.7	10/6/2008	113.8	4/20/2009	114.2
3/5/2007	114.0	9/17/2007	115.4	3/31/2008	114.6	10/13/2008	113.8	4/27/2009	114.5
3/12/2007	114.6	9/24/2007	115.7	4/7/2008	115.1	10/20/2008	113.8	5/4/2009	114.4
3/19/2007	114.1	10/1/2007	114.7	4/14/2008	115.3	10/27/2008	114.0	5/11/2009	114.4

Appendix 2 Gas Generation: Total Pressure (continued)

Date	Pressure (kPa)	Date	Pressure (kPa)	Date	Pressure (kPa)	Date	Pressure (kPa)	Date	Pressure (kPa)
5/18/2009	114.7	12/7/2009	115.2	6/28/2010	114.3	1/17/2011	112.0	8/8/2011	114.0
5/25/2009	117.9	12/14/2009	115.2	7/5/2010	114.4	1/24/2011	112.1	8/15/2011	114.0
6/1/2009	118.3	12/21/2009	113.9	7/12/2010	114.2	1/31/2011	112.1	8/22/2011	114.0
6/8/2009	118.1	12/28/2009	113.8	7/19/2010	114.2	2/7/2011	112.1	8/29/2011	114.0
6/15/2009	117.5	1/4/2010	113.6	7/26/2010	114.0	2/14/2011	112.3	9/5/2011	114.1
6/22/2009	114.5	1/11/2010	113.9	8/2/2010	113.8	2/21/2011	112.5	9/12/2011	114.1
6/29/2009	114.4	1/18/2010	114.1	8/9/2010	113.7	2/28/2011	112.3	9/19/2011	114.3
7/6/2009	114.2	1/25/2010	113.7	8/16/2010	113.9	3/7/2011	112.7	9/26/2011	114.7
7/13/2009	114.5	2/1/2010	113.6	8/23/2010	113.8	3/14/2011	112.7	10/3/2011	114.8
7/20/2009	114.6	2/8/2010	115.4	8/30/2010	113.7	3/21/2011	112.8	10/10/2011	114.8
7/27/2009	114.6	2/15/2010	114.4	9/6/2010	113.9	3/28/2011	112.6	10/17/2011	115.1
8/3/2009	114.7	2/22/2010	114.1	9/13/2010	113.9	4/4/2011	112.6	10/24/2011	114.9
8/10/2009	114.5	3/1/2010	114.1	9/20/2010	113.8	4/11/2011	112.5	10/31/2011	114.7
8/17/2009	114.4	3/8/2010	113.9	9/27/2010	114.7	4/18/2011	112.5	11/7/2011	114.8
8/24/2009	114.6	3/15/2010	114.1	10/4/2010	113.6	4/25/2011	112.8	11/14/2011	114.8
8/31/2009	114.3	3/22/2010	113.8	10/11/2010	113.2	5/2/2011	112.9	11/21/2011	114.8
9/7/2009	114.3	3/29/2010	113.7	10/18/2010	113.2	5/9/2011	113.0	11/28/2011	114.6
9/14/2009	114.2	4/5/2010	113.6	10/25/2010	113.4	5/16/2011	112.8	12/5/2011	114.7
9/21/2009	115.3	4/12/2010	113.6	11/1/2010	114.6	5/23/2011	112.6	12/12/2011	114.8
9/28/2009	115.7	4/19/2010	113.5	11/8/2010	114.9	5/30/2011	112.6	12/19/2011	114.6
10/5/2009	115.4	4/26/2010	113.5	11/15/2010	115.2	6/6/2011	112.6	12/26/2011	
10/12/2009	115.4	5/3/2010	113.5	11/22/2010	115.3	6/13/2011	112.8	1/2/2012	114.7
10/19/2009	115.2	5/10/2010	113.6	11/29/2010	113.1	6/20/2011	113.0	1/9/2012	114.9
10/26/2009	115.4	5/17/2010	113.9	12/6/2010	111.9	6/27/2011	113.2	1/16/2012	115.0
11/2/2009	115.3	5/24/2010	114.2	12/13/2010	112.1	7/4/2011	112.8	1/23/2012	117.7
11/9/2009	115.3	5/31/2010	114.3	12/20/2010	111.9	7/11/2011	113.1	1/30/2012	116.6
11/16/2009	115.2	6/7/2010	114.2	12/27/2010	111.8	7/18/2011	113.0	2/6/2012	116.5
11/23/2009	115.3	6/14/2010	114.2	1/3/2011	111.9	7/25/2011	113.7	2/13/2012	116.5
11/30/2009	115.1	6/21/2010	114.1	1/10/2011	112.0	8/1/2011	113.8	2/20/2012	116.4

Appendix 2 Gas Generation: Total Pressure (continued)

Date	Pressure (kPa)	Date	Pressure (kPa)	Date	Pressure (kPa)	Date	Pressure (kPa)	Date	Pressure (kPa)
2/27/2012	116.1	9/17/2012	118.0						
3/5/2012	114.8	9/24/2012	117.7						
3/12/2012	114.8	10/1/2012	117.9						
3/19/2012	114.6	10/8/2012	117.8						
3/26/2012	114.5	10/15/2012	117.6						
4/2/2012	114.2	10/22/2012	118.1						
4/9/2012	114.2	10/29/2012	117.8						
4/16/2012	114.2	11/5/2012	118.0						
4/23/2012	114.2	11/12/2012	117.8						
4/30/2012	114.1	11/19/2012	117.8						
5/7/2012	115.4	11/26/2012	117.8						
5/14/2012	116.2	12/3/2012	117.8						
5/21/2012	116.1	12/10/2012	116.8						
5/28/2012	116.9	12/17/2012	116.2						
6/4/2012	116.8	12/24/2012	116.7						
6/11/2012	117.4	12/31/2012	117.1						
6/18/2012	117.2	1/7/2013	117.0						
6/25/2012	117.5	1/14/2013	117.1						
7/2/2012	117.3	1/21/2013	117.0						
7/9/2012	117.0	1/28/2013	118.0						
7/16/2012	117.6								
7/23/2012	117.6								
7/30/2012	117.7								
8/6/2012	117.6								
8/13/2012	117.8								
8/20/2012	117.7								
8/27/2012	117.5								
9/3/2012	118.1								
9/10/2012	118.2								

Appendix 3: Photographs of the SSR inner bucket

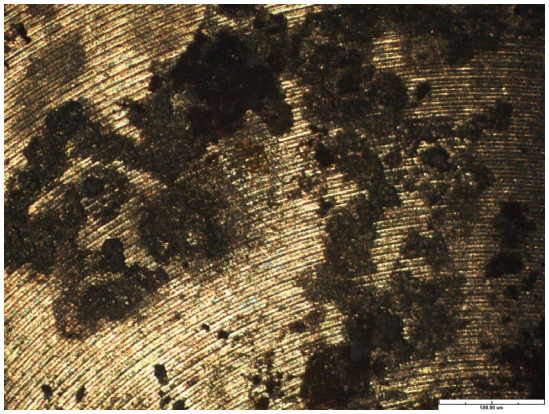

Bottom

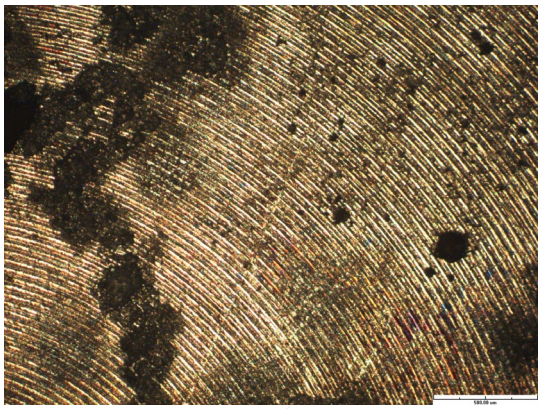

Bottom

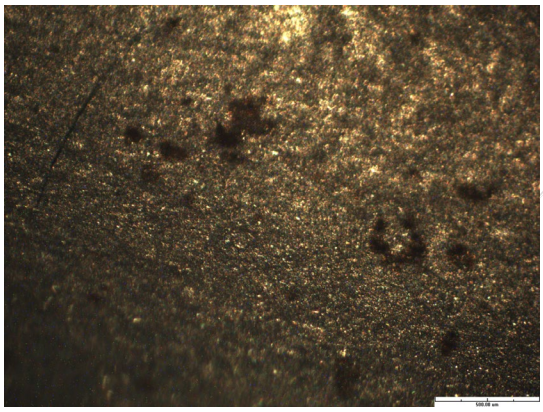

Side Wall: Near Bottom

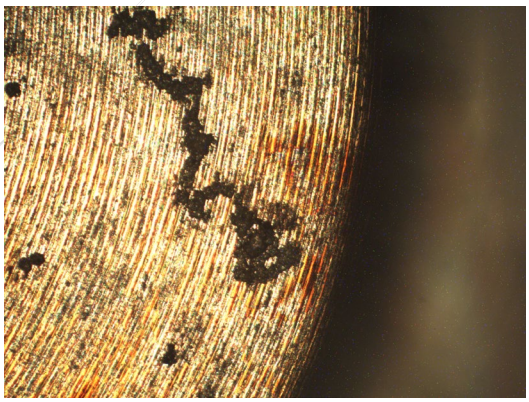

Bottom

Appendix 4: Estimating the monolayer coverage

Surface Area: The number of monolayers of moisture on the sample surface may be calculated if the mass of moisture or water, the mass of the sample, and the SSA of the sample are known. One approach is to determine the weight percentage for one monolayer of water. The number of monolayers of water can be calculated by dividing the total weight percentage of water (mass of water/mass of the sample) by the weight percentage of one monolayer of water.[12] The weight percentage of one monolayer of water is the product of the weight of water in a monolayer of 1 m^2 and the SSA:

$$\text{wt\% of 1 ML} = 0.00022\ \text{g m}^{-2}\text{ML}^{-1} \times \text{SSA m}^2\ \text{g}^{-1} \times 100\text{wt\%}$$

$$= .022\text{wt\% ML}^{-1} \times \text{SSA.} \qquad \text{Equation A1-1}$$

For the material MT1490 with a SSA of 0.84 m^2 g^{-1} (calculated from the weighted averages of the measured SSAs), the weight percentage of one monolayer of water is 0.0185wt% ML^{-1}.

Dividing the weight percentage of water by the weight percentage of water in one monolayer yields the number of monolayers of water. Applying this to the measured weight percentage of water upon loading and unloading results in:

Loading Condition: 0.40 wt% / 0.0185wt% ML^{-1} = 21.6 ML

Unloading Condition: 0.15 wt% / 0.031wt% ML^{-1} = 8.1 ML

BET Theory: The number of monolayers can also be estimated based upon the relative humidity (RH) in the container using Brunauer-Emmett-Teller (BET) theory.[8] BET theory is the standard model for quantifying the equilibria between multiple physically adsorbed layers on a surface and the adsorbing species in the gas above the surface. The specific relationship between the RH above a surface and the number of monolyers of weakly bound water on the surface predicted by BET theory is illustruated in Fig. A-1 for several values of c.

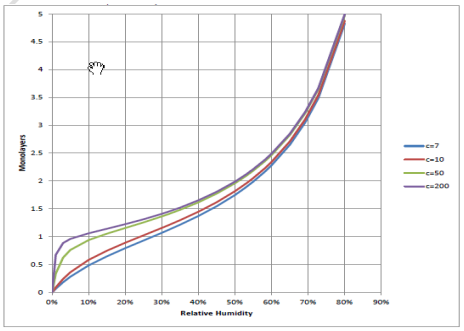

Figure A-1. Adsorption Isotherm Calculated from BET Theory.

The equation for calculating the number of monolayers at a given RH and c value is given in Equation A1-2.

$$c*RH/100/(1-RH/100)[1+(c-1)RH/100] \qquad \text{Equation A1-2}$$

Appendix 5: Stopping power ratio

The ratio of the stopping power due to the water and the stopping power due to the material is calculated using the approach in Appendix B of Reference 6.

Species	**Integrated at 5.2MeV**		**MT1490**	
H2O(g)	7.946		0.0000	0
H2O (l)	7.708		0.0040	0.03083
F	6.645		0.0000	0
O	5.901		0.0000	0
Na	5.304		0.0000	0
C	5.190		0.0000	0
S	5.117		0.0000	0
Mg	5.100		0.0000	0
Si	4.852		0.0000	0
Al	4.702		0.0000	0
K	4.652		0.0000	0
Cl	4.575		0.0000	0
Ca	4.461		0.0000	0
Cr	3.688		0.0000	0
Fe	3.504		0.0000	0
Ni	3.184		0.0000	0
Cu	2.871		0.0000	0
Zn	2.860		0.0000	0
Ga	2.786		0.0000	0
UO2	2.081		1.0000	2.08

Smat	2.083
Swat	7.71
S	**3.70**

Appendix 6: Obtaining G-values and rate constants

As discussed in the H2 G-value and rate constants section, a double exponential growth function fits the time dependence of the partial pressure curve for hydrogen in many of the MIS studies. The double exponential has three fitting parameters, A_0, the initial active water, k_1 the hydrogen formation rate constant and k_2, the hydrogen consumption rate constant. These fitting parameters can be used along with information of material properties and container geometry to calculate the initial rate, the hydrogen G-value, and empirical rate constants. This appendix documents the methodology for obtaining this information.

Calculation of *G(H₂)*

G(H₂) can be calculated by equating the initial rate of hydrogen generation to the product of the rate of dose to the water and *G(H₂)*,

$$\frac{dN_{H_2}}{dt} = \dot{D}_{H_2O}\, G(H_2)$$

Equation A6-1

where N_{H2} is the number of molecules of hydrogen and $\dot{D}_{H2O}$ is the rate of adsorbed dose to the water with units eV s^{-1}. The initial rate is given by the differential

$$\frac{dP_{H2}}{dt} = k_1\, A_0 e^{-k_1 t} - k_2 P_{H2}$$

evaluated at time zero in units of molecules per second rather than kPa per day, given P_{H2} is zero at t = 0.

$$\left.\frac{dP}{dt}\right]_{t=0} = k_1\, A_0\, e^{-bt}]_{t=0} = k_1\, A_0$$

$$\frac{dN_{H_2}}{dt} = \frac{dP}{dt}\,\frac{V_g\, N_A}{R\, T} = k_1\, A_0\,\frac{V_g\, N_A}{R\, T}\,\frac{day}{86400\, s}$$

$$k_1\, A_0\,\frac{V_g\, N_A}{R\, T}\,\frac{day}{86400\, s} = \dot{D}_{H_2O}\, G(H_2)$$

Equation A6-2

In Equation , V_g is the gas volume within the reactor, N_A is Avogadro's number, R is the universal gas constant, T is the temperature in the gas phase during the time the data was collected. The method for calculating V_g within an SSR is shown in the Loading section. The dose rate to the water is given by

$$\dot{D}_{H_2O} = P_{mat}\ \frac{6.2418\ \text{x}\ 10^{18}\ \text{eV}}{\text{s W}}\ m_{mat}\ f_{H_2O}\ \frac{S_{H_2O}}{S_{mat}}$$

$$f_{H_2O} = \frac{m_{H_2O}}{m_{mat}}$$

$$\dot{D}_{H_2O} = P_{mat}\ \frac{6.2418\ \text{x}\ 10^{18}\ \text{eV}}{\text{s W}}\ m_{H_2O}\ \frac{S_{H_2O}}{S_{mat}}$$

Equation A6-3

where P_{mat} is the specific power of the material in W g^{-1}, m_{mat} is the mass of the material, f_{H2O} is the fraction of water, and the ratio S_{H2O}/S_{mat} is the ratio of the stopping power of alpha particles in water to the stopping power in the material. An approach for calculating S_{H2O}/S_{mat} is given in Appendix B. For high-purity plutonium dioxide with adsorbed water and no impurities the ratio S_{H2O}/S_{mat} for 5.2 MeV α-particles is ~3.70. Combining Equation and Equation A6-3 yields a general expression for $G(H_2)$ using the fitting parameters a and b, and the material properties,

$$G(H_2) = k_1\ A_0\ \frac{V_g N_A}{R\ T}\ \frac{day}{86400\ s}\ \frac{1}{P_{mat}\ \frac{6.2418\ \text{x}\ 10^{18}\ \text{eV}/100}{\text{s W}}\ m_{H_2O}\ \frac{S_{H_2O}}{S_{mat}}}$$

Equation A6-4

Conversion of rate constants

The initial formation rate constant, $\boldsymbol{k_{for}}$, can be expressed in terms of molecules of hydrogen produced per second of active water using the equations below.

$$k_{for} = k_1 A_0 \frac{V_g N_A}{R\ T}\ \frac{day}{86400\ s}$$

Equation A6-5

The consumption rate constant, k_2, expressed in units of days^{-1}, can be expressed in terms of molecules of hydrogen consumed per second per kPa of hydrogen using the equations below.

$$k_{con} = k_2 \frac{V_g N_A}{R\ T}\ \frac{day}{86400\ s}$$

Equation A6-6

Appendix 6: Obtaining G-values and rate constants (continued)

Calculation of rate constants for surface catalyzed decomposition of water to form H_2

The surface catalyzed decomposition of water to form H_2 has been proposed by Haschke and co-workers.[13] The reaction is described by,

$$PuO_2(s) + xH_2O(ads.) \longrightarrow PuO_{2+x}(s) + x\,H_2(g) \qquad \text{Equation A6-7}$$

The reaction "contributes to H_2 pressurization of sealed storage containers until the equilibrium pressure of Equation A5-7 is reached."[13a] The amount of solid plutonium dioxide and water is large compared to the amount of H_2 and higher oxide produced. The initial reaction rate will be essentially constant throughout the reaction. The H_2 consumption reaction, in this case a true back reaction, is first order in H_2 partial pressure and in the amount of the higher oxide. The rate was found to be independent of adsorbed water over a wide range of adsorbed water. The observed initial rate of formation is divided by the total surface area of the material to obtain values that can be compared to Haschke's reaction rates,

$$R_{for} = A_0 k_1 \frac{day}{24\,hr} \frac{V_g}{R\,T} \frac{1}{SSA\,m_{mat}} \qquad \text{Equation A6-8}$$

where *SSA* is the specific surface area of the material and m_{mat}.is the mass of the plutonium dioxide. This formation rate, R_{for}, is expressed in units of moles m^{-2} hr^{-1} kPa^{-1} of active water. The rate of the surface catalyzed consumption reaction is given by

$$R_{con} = k_2 \frac{day}{24\,hr} \frac{V_g}{R\,T} \frac{1}{SSA\,m_{mat}} \quad . \qquad \text{Equation A6-9}$$

Appendix 7: Symbols and Conversion Factors

Symbols

Symbol	Units	Description
A	kPa	Active water or the water involved in hydrogen generation
A_0	kPa	Initial active water (fitting parameter)
k_1	day^{-1}	Rate constant for the formation of hydrogen from water (fitting parameter)
k_2	day^{-1}	Rate constant for the consumption of hydrogen (fitting parameter)
$\dot{D}_x$	eV s^{-1} or J s^{-1} or W	Rate of adsorbed dose to x
G(x)	molecules 100 eV^{-1}	Number of molecules of x produced per 100 eV of adsorbed dose
f_x	---	Fraction of material x in the total material
m_x	g	Mass of x
N_x	molecules	Number of molecules of substance x
N_A	molecules mol^{-1}	Avogadros number
p_x	kPa	Partial pressure of x
P_x	W g^{-1} or eV s^{-1} g^{-1}	Specific power of x
S_x	m	Stopping power of x to alpha radiation
SSA	m^2 g^{-1}	Specific Surface Area of the material
t	s or day or yr	Time
T	K	Temperature
V_g	cm^3	Volume that the gas occupies

Appendix 7: Symbols and Conversion Factors (continued)

Unit conversions

1 W	6.2418×10^{18} eV s^{-1}
1 day	86400 s
1 day	24 hr
N_A	6.0221367×10^{23} molecules mol^{-1}
R	8.314510 J mol^{-1} K^{-1} 8.314510 kPa L mol^{-1} K^{-1} 8314.510 kPa cm^3 mol^{-1} K^{-1}